

Model Estimates of Traffic Reduction in Storm Impacted En Route Airspace[†]

Brian D. Martin*

Massachusetts Institute of Technology, Lincoln Laboratory, 244 Wood Street, Lexington, MA 02420

An understanding of convective weather impacts on en route airspace capacity is a first step toward development of predictive tools to support both tactical and strategic routing decisions in storm-impacted airspace. This study presents a model for traffic reductions in en route sectors that result from convective weather impacts. A model to predict the impact of convective weather on en route traffic, Traffic Normalized Fractional Route Availability (TNFRA), combines Weather Avoidance Fields (WAF) from the Convective Weather Avoidance Model (CWAM) with a model for route usage in air traffic control (ATC) sectors. The model estimates the number of flights that will be able to pass through convective weather in a given sector. Results show that TNFRA provides a relatively unbiased estimate of sector traffic when compared to actual operations during high impact – convective weather events.

I. Introduction

The goal of integrating weather and Traffic Flow Management (TFM) at the Air Traffic Control (ATC) sector level begins with the development of models relating operational impacts in en route airspace to convective weather. This paper presents the Traffic Normalized Fractional Route Availability (TNFRA) model, which combines Weather Avoidance Fields (WAF) from the Convective Weather Avoidance Model¹ (CWAM) with a model for route usage in air traffic control (ATC) sectors to estimate the number of flights that will be able to pass along a route through convective weather in the sector.

TNFRA estimates sector capacity as a traffic-weighted sum of the ‘passability’ of all routes in the sector. It assumes that traffic may deviate only within the operational boundaries of the defined routes, where the operational boundaries are determined by route density and the observed limits of deviation along those routes. By retaining the constraints of the underlying route structure, TNFRA avoids the need to account for the increase in complexity and workload that arises when traffic must be routed in novel ways³. However, TNFRA could be applied to more general ‘flow-based’ models (e.g., Mitchell⁴, Song⁵, Hunter⁶), as long as proper care is taken to account for the capacity impact due to the additional complexity and workload required to implement less structured traffic flows.

Traffic estimates have been calculated for the 406 low, high, and super-high ATC sectors bounded by the current Corridor Integrated Weather System² (CIWS) domain. Each ATC sector’s airspace is defined by a volume of airspace with a polygonal cross section, specific floor and ceiling altitudes and contains a set of defined jet routes. CIWS weather inputs are employed to generate WAFs that are used to model the impact of a given weather event on the traffic of each sector. Results show that TNFRA provides a relatively unbiased estimate of the traffic reduction experienced in ATC sectors during convective weather events.

*Technical Staff, Massachusetts Institute of Technology, Lincoln Laboratory, Group 43 Weather Sensing

[†]This work was sponsored by the National Aeronautics and Space Administration (NASA) under Air Force Contract FA8721-05-C-0002. Opinions, interpretations, conclusions, and recommendations are those of the authors and are not necessarily endorsed by the United States Government.

II. Methodology

A. Meteorological Data Input

The WAF is a gridded field that provides an estimate of pilot deviation probability (WAF-pdps) at each pixel in the grid as a function of VIL, echo top height and flight altitude. WAFs were calculated using VIL and echo top products from CIWS, which have a horizontal resolution of 1 km x 1 km over the CIWS domain and an update rate of 5 minutes. WAFs were calculated for en route flight altitudes of 27 kft, 31 kft, 35 kft, and 39 kft. WAF-pdps are output in discrete bins from 0% to 100% at a 10% probability interval. Figure 1 illustrates the conversion of CIWS weather data into WAF-pdps.

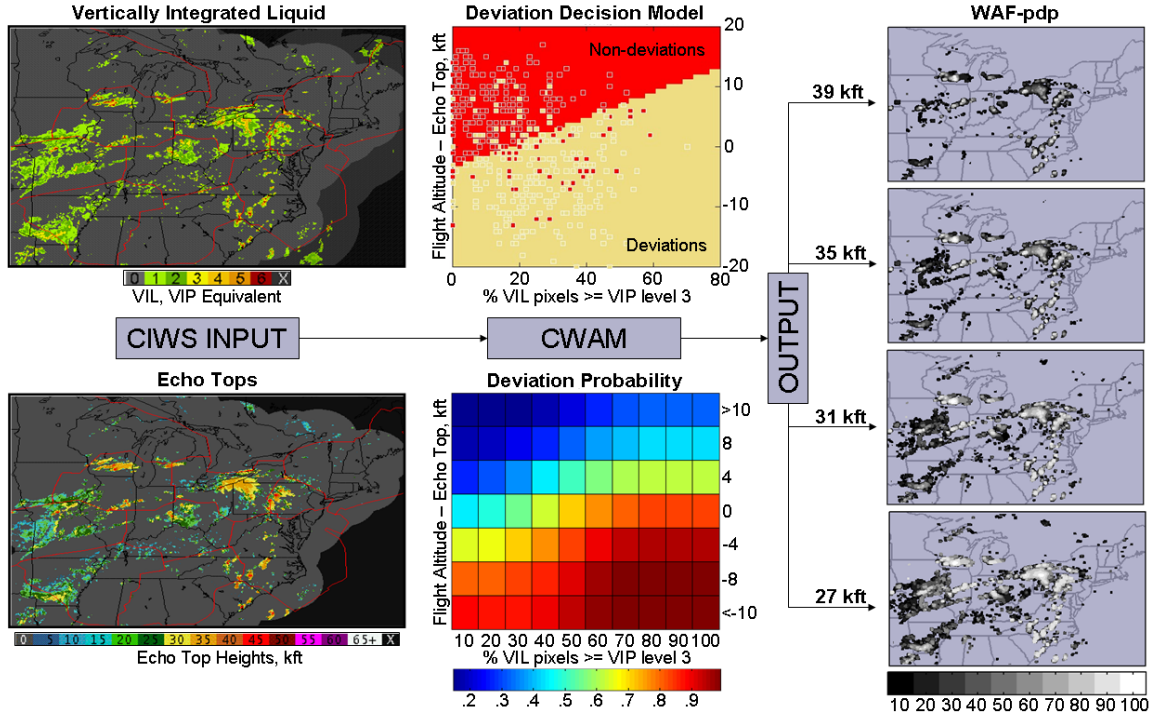


Figure 1. Flow chart for the generation of Weather Avoidance Field pilot deviation probabilities.

B. ATC sector Data Inputs

In en route airspace, the NAS is divided into ATC sectors, giving controllers a 3-D portion of airspace for which they are responsible. Each ATC sector is defined as a volume of airspace with polygonal cross section, specific floor and ceiling altitudes that contains a set of defined jet route segments. ATC sector geospatial data used in this study was provided by the Enhanced Traffic Management System (ETMS). Figure 2 illustrates the high altitude sector ZOB48 and the complex jet route structure (total of 11 jet routes) that carries the majority of ZOB48 traffic. Gray vertical planes indicate the center location of the jet routes. The jet routes are used in combination with WAF-pdps to assess convective weather impacts on traffic within the sector. A similar structure of sector boundaries and routes is used for each of the 406 low, high and super-high altitude sectors bounded by the CIWS domain.

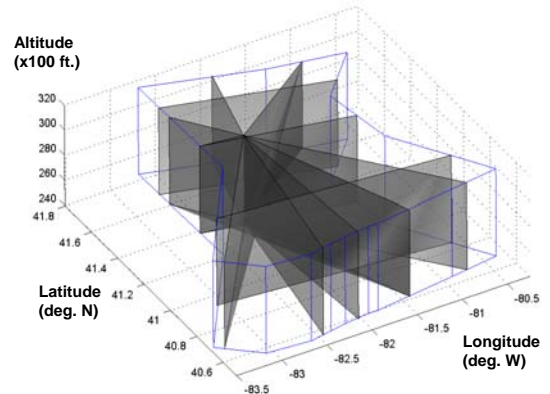


Figure 2. Geospatial location of ZOB48 and associated jet route center planes.

C. ATC sector Route Availability (RA) Algorithm

Estimates of sector capacity are derived from a calculation of a sector's route availability (RA). RA is based on the spatial intersection of the route with the WAF (27, 31, 35, or 39 kft.) whose altitude is closest to the ATC sector's center altitude. In cases where the ATC sector has an unbounded ceiling altitude, the central altitude between the floor and 42kft is used.

WAF-pdps are initially converted into a binary obstruction field by initially defining an obstruction as a pixel whose probability of deviation is 80% or greater. Through this constructed binary obstruction field, we attempt to find a traversable path within the bounds of a given route. If no traversable path is found through the 80% obstruction field, the 90% then 100% WAF-pdp obstruction fields are constructed and searched. If no path is found through the obstructed field, the route is considered blocked and RA for that particular route is set to zero.

In order to find a traversable path, the route is divided into a series of route segments of parameterized length. For this exercise we used a segment length of 55km (~30 nm), consistent with en route mile in trail restrictions set in airspace impacted by convective weather⁷. Figure 3a shows segmentation of an example route (bounded by the black vertical lines). Route widths are also parameterized and are currently set to 40 km (~20nm), representative of the median deviation distances observed of en route transits¹. Complexity of the traversable path output is controlled by the adjustment of the segment length and width parameters, for instance, to model different degrees of automation, aircraft performance or air traffic control airspace usage models.

Each route segment is further divided across its width into a series of 1km wide sub-segments that run the length of the route segment. Sub-segments are bounded by red horizontal lines in the route example of Fig. 3. A sub-segment that does not contain an obstruction pixel (black ovals in Fig. 3b) is considered traversable (green highlighted sub-segments of Fig. 3b). Any collection of adjacent traversable sub-segments in a route segment defines an unobstructed pathway through the segment.

The traversable path algorithm searches the set of unobstructed sub-segments for obstruction-free paths that traverse the ATC sector. For each of the paths found, the minimum path width is computed. The traversable path chosen for the route availability calculation is the obstruction-free path with the greatest minimum width (Fig. 3c). Once this traversable path is found, the 'choke point' is identified at the center of the traversable path at the narrowest point (indicated by the red diamond in Fig. 3c).

Given a traversable path along a route, RA is defined as the complement of the distance-weighted average WAF-pdp of pixels in the region bounded by the two segments sharing a coterminous border with the choke point, where the distance used is the radial distance from the choke point. Figure 4 provides an example of the RA assessment on the portion of J146 (green box) bounded by ZOB49, a super-high altitude sector of the Cleveland (ZOB) Air Route Traffic Control Center (ARTCC). Figure 4a shows the VIL field and 35 kft. echo top contour. Figure 4b shows the WAF-pdp field, the traversable path (green) and choke point (red diamond) for J146. The distance weighted average WAF-pdp, calculated from the pixels in the two middle route segments (those on either side of the choke point) is 0.41; the RA for J146 is $1.00 - 0.41 = 0.59$.

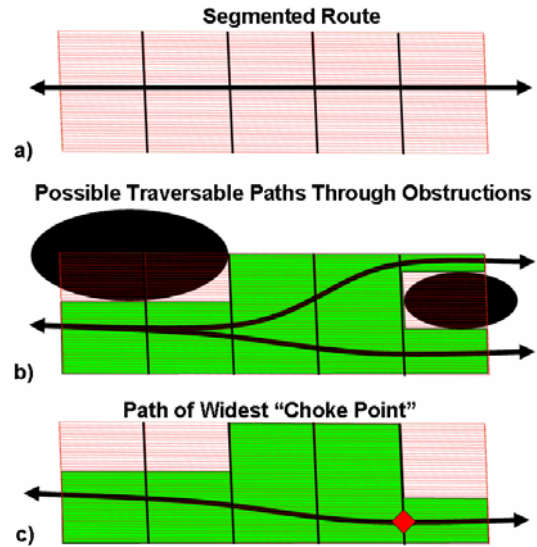


Figure 3. Finding the traversable path along a route through an obstructed field. Traffic flow direction indicated by arrows where a) shows route segmentation, b) shows possible unobstructed paths, and c) shows the chosen path with widest "choke point".

Cleveland Center Sector: ZOB 49, Route J146

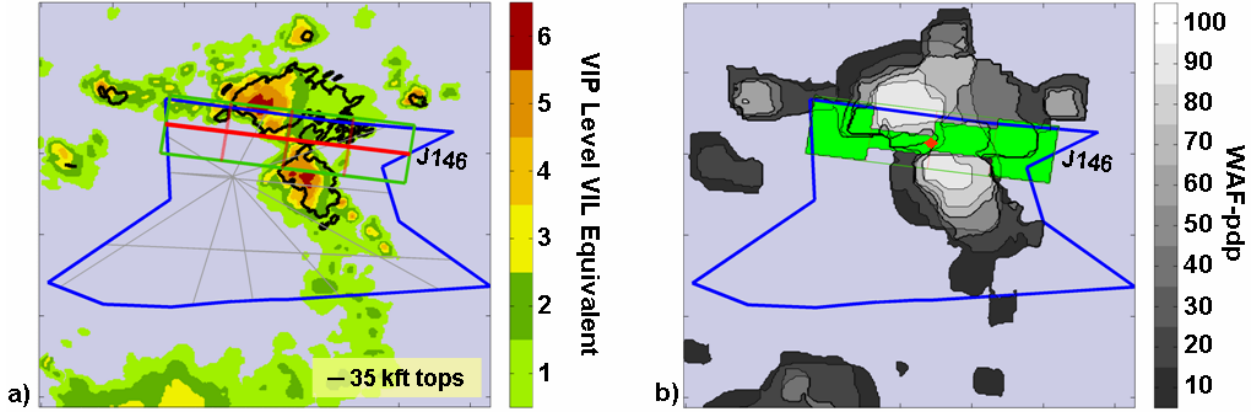


Figure 4. Example of weather impacts on super high altitude sector ZOB49 of the Cleveland Center ARTCC. a) Echo tops and VIL depict a line of convective cells affecting routes in ZOB49. b) Traversable path calculated for jet route J146 (highlighted solid green) given the generated WAF-pdp of weather depicted in a. The red diamond in the traversable path indicates the “choke point” center where J146 RA is calculated.

D. Calculating Sector Impacts using Route Availability

Convective weather that blocks low-traffic routes has less impact on air traffic than weather that blocks busy routes. Since the traffic on routes within a sector varies significantly with time, a route that typically handles little traffic at a time of convective weather impact should not be weighted the same as a heavily used route in the estimation of weather impact on sector capacity. The TNFRA sector impact metric accounts for traffic load by weighing the RA for each route i at some time t by its typical fair-weather traffic at that time (defined below in Eq. 1 as $\text{FWT}(t)_i$):

$$\text{TNFRA}(t) = \frac{\sum[(\text{RA}(t)_i) \text{FWT}(t)_i]}{\sum \text{FWT}(t)_i} \quad (1)$$

To determine $\text{FWT}(t)_i$ for each route in a sector, minute-by-minute traffic counts were generated using ETMS data and averaged over three storm-free weekdays. Figure 5 illustrates the fair-weather traffic counts for each route segment near the time of peak traffic demand in the overall CWIS domain.

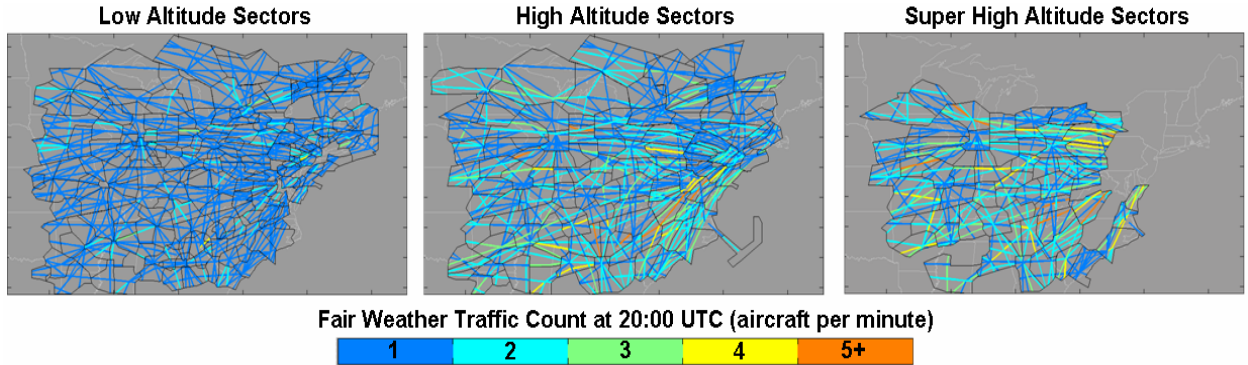


Figure 5. Fair weather traffic profiles for routes in low, high and super-high altitude sectors of the CIWS domain. Route profiles provide weights for the TNFRA estimate of weather impact on an ATC sector.

III: Results

Impact estimates were calculated for a convective weather event that occurred on 27 July 2006. This event had a widespread and time-extended impact on the NAS. The ZOB ARTCC was a major focal point for many of the delays, reroutes, and ground stops that occurred between 1:00 UTC on the 27th to 1:00 UTC on the 28th. Ground stops at airports in the northeast (including airports in Philadelphia and in New York) were directly related to jet routes in ZOB being completely unavailable. Figure 6 includes color maps of TNFRA for ATC sectors in ZOB near the time of peak storm impact on air traffic (19:00 UTC 27 July 2006). The figure also includes a grayscale overlay of WAF-pdps and the 80% WAF-pdp contour (in white), both corresponding to the altitude layer nearest the average center altitude of the sectors in the image (from left to right, WAF altitudes of 27kft, 31Kft, and 35kft are shown). The color coded TNFRA estimates for low (left), high (center), and super high (right) sectors indicate significant reductions in the eastern portion of ZOB at low and high levels. At the super high flight levels, ZOB59 (orange sector in far right) is the only super high sector showing significant impact. The increased route availability at the super high altitude layer is directly attributed to the dependence of WAF deviation probabilities on the difference between flight altitude and echo top height. The high altitude sectors along the eastern boarder of ZOB are responsible for much of the traffic into and out of New York and Philadelphia where ground stops and delays resulted in much of the gridlock experienced during the event[†].

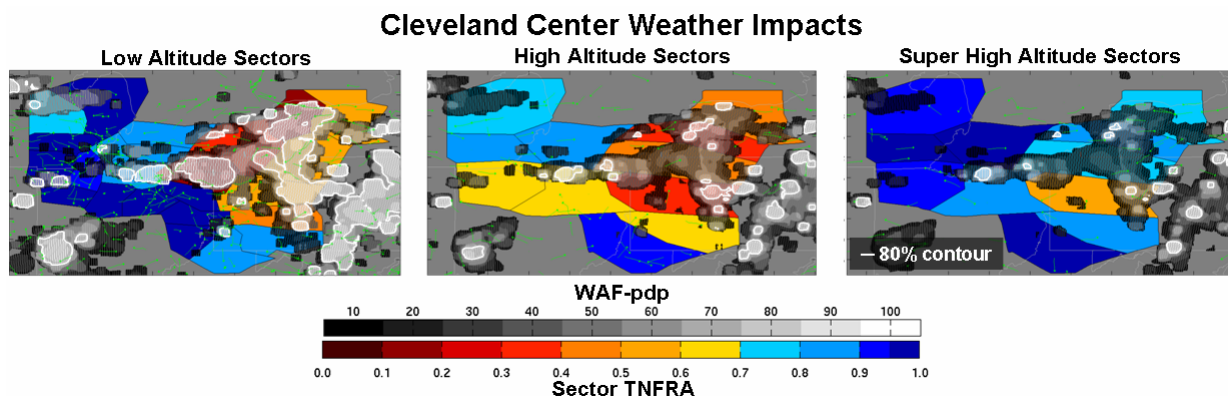


Figure 6. Example of Cleveland Center (ZOB) weather impacts as calculated using WAF-pdps and TNFRA at 19:00 UTC 27 July 2006. White contours indicate the 80% WAF-pdp for each level. TNFRA estimates for low (left), high (center), and super high (right) ATC sectors have been color coded from low impact (blue) to high impact (red).

A. TNFRA Estimates Compared to Actual Sector Traffic

TNFRA estimates spanning the 24 hour event were derived at a one minute time step for all ATC sectors bounded by the CIWS domain (406 sectors in total). This provides a data set of 584,640 TNFRA estimates to compare to the actual sector route usage during the 27 July 2006 convective event. To evaluate overall accuracy of the TNFRA algorithm, the histograms of figure 7 compare the one-minute sector TNFRA estimates to the actual ETMS sector traffic counts during the 27 July event. TNFRA estimates for each sector are rounded to the nearest integer. The histogram bin amplitudes represent the number of instances for which the difference between a sector's actual count and its TNFRA estimate equaled a specific integer value (Δ). Positive Δ indicates that TNFRA overestimated the weather impact on a sector at any given time, negative Δ indicates an underestimate. The first histogram in Fig. 7 shows the occurrence distribution of these differences over all 312,705 instances in which the ATC sector average non-normalized route availability (\overline{RA}) indicated any weather impact at all on a sector ($\overline{RA} < 1$). The following histograms examine smaller sets of instances with more severe weather impact (ATC sector $\overline{RA} < 0.75$, $\overline{RA} < 0.50$, and $\overline{RA} < 0.25$).

The results show that TNFRA provides a relatively unbiased estimate of the impact of convective weather on sector traffic. The histogram for the any weather impact cases ($\overline{RA} < 1$) has only a slight positive skew, with only 5% more non-zero Δ 's registering as overestimates of weather impact on traffic. As \overline{RA} decreases, TNFRA overestimates storm impact more frequently and the distribution becomes more positively skewed. However, even in cases with \overline{RA} less than 0.25 where overestimates of the weather impact make up 81% of nonzero Δ , the median

[†] See the FAA Advisories Database made available at <http://www.fly.faa.gov/AdvisoryForm.jsp> [cited Sept. 14, 2007]

remains zero and no increase in the upper quartile range is observed ($q_{0.75}$ is equal to 1.0 for all $\overline{RA} < 1.0$ comparisons).

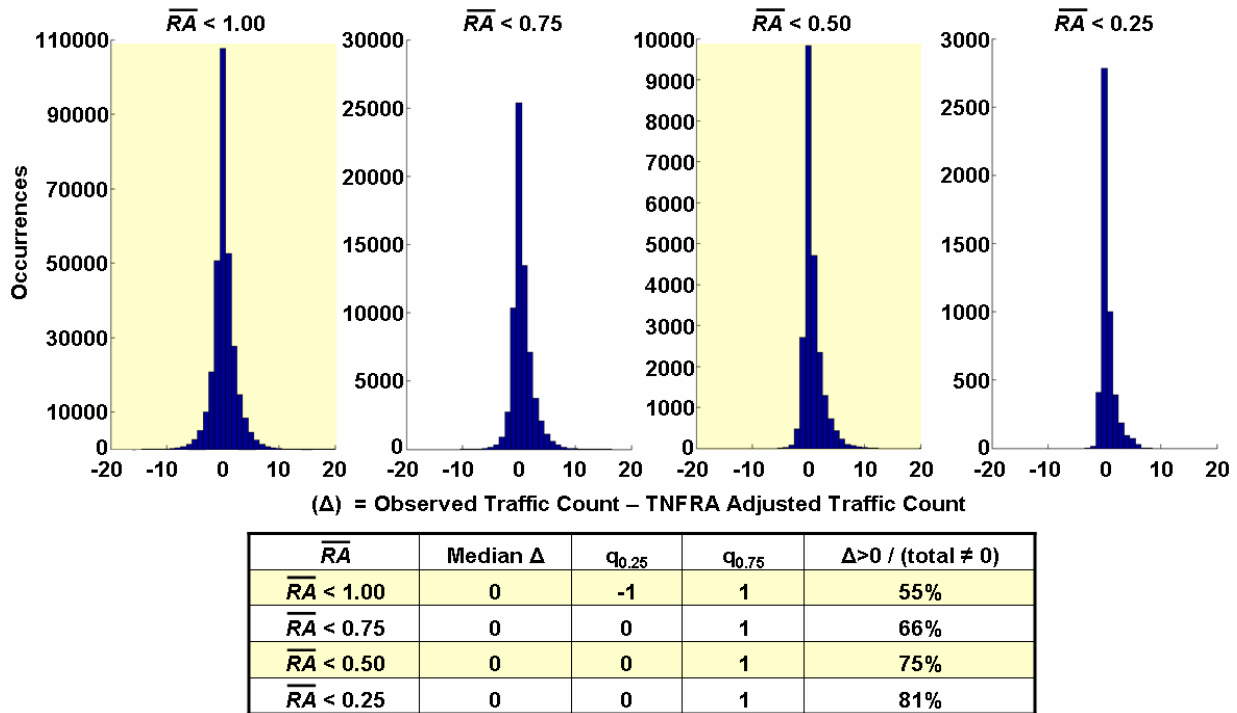


Figure 7. Comparison of TNFRA estimated one minute traffic counts and actual observed one minute traffic counts for 27 July 2006 convective weather event.

In the tails of the distributions, instances do occur where Δ exceeds roughly 10 aircraft in either direction. Although these Δ are large relative to typical sector capacities, they are relatively rare. Tails of the Δ distributions are largely due to the fact that TNFRA focuses only on established routes (deviations beyond the bounds of the defined routes are not allowed in the route availability calculations), does not account for variations from fair weather demand caused by controller actions (reroutes, ground stops, etc.) and estimates sector availability on a local scale without accounting for conditions in surrounding sectors.

TNFRA will over-estimate ($-\Delta$) useable capacity when blockages occur in up-stream sectors, prohibiting traffic from reaching an unobstructed sector. Figure 8 is an example of such an instance in the New York Center high altitude sector ZNY42. The fair-weather traffic snapshots shown in a, b, and c at 19:05 UTC show that ZNY42 regularly operates at an instantaneous count of about seven aircraft (white trajectories in figure a, b, and c). Figure 8d shows a snapshot where traffic within ZNY42 is indirectly affected by convective activity. No convective weather is present within the bounds of ZNY42; hence, TNFRA route availability in the sector is 1. However, in sectors directly to the west of ZNY42, convective weather has significantly reduced the route availability. Flow blockage from weather impacts on the red sectors west of ZNY42 led to ground stops at New York and airports to the south that reduced the actual aircraft count in ZNY42 to zero, even though the sector's interior route structure is not experiencing weather impacts.

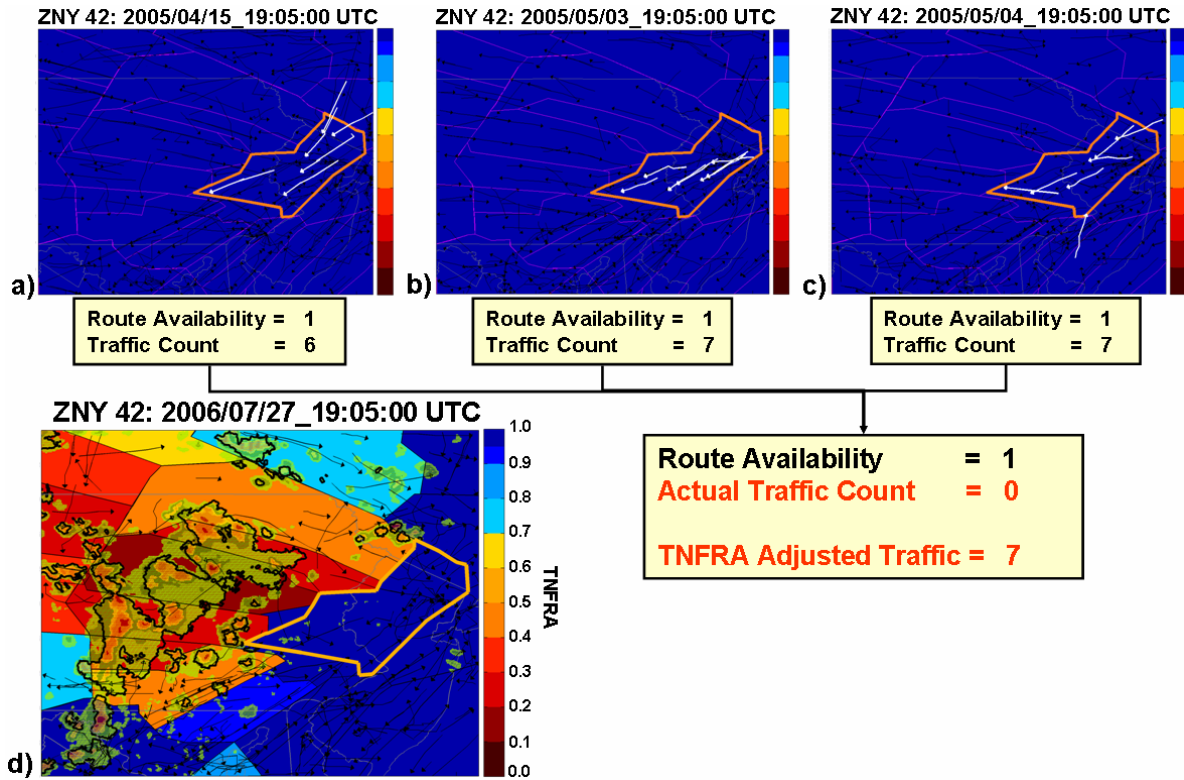


Figure 8. Differences in the demand profile of ZNY42 during the three fair weather days of a), b), and c) used to create sector traffic profiles and d) the 27 July 2006 high impact event. White trajectories in each plot indicate aircraft under responsibility of controllers in ZNY42, black trajectories show aircraft outside or below ZNY42 airspace. Note while in each circumstance RA is 1.00, surrounding impacts at 20060727_19:05:00 UTC reduce demand on ZNY42 by 100% when compared to use on fair weather days.

TNFRA can overestimate impacts on capacity when controllers and managers have space to vector traffic around storms or are able to shift flow to unobstructed routes or sectors. These effects are reflected in the positive values of the Δ distributions in Fig. 7. An example of this exploitation of unobstructed airspace within a sector is illustrated in figure 9, which shows TNFRA estimates for ZAU60, a large high-altitude sector of the Chicago ARTCC, at 19:12 UTC of the 27 July event. Figure 9a illustrates the average fair weather traffic flows at 19:12 UTC. Traffic flow is concentrated on major jet routes J36 and J68, with little to no traffic along the north-south routing options. Given the fair weather estimate of sector use at 19:12 UTC, ZAU60 typically operates at an instantaneous traffic count of 10 aircraft. A large exploitable section of airspace lies to the north of ZAU60's major axis.

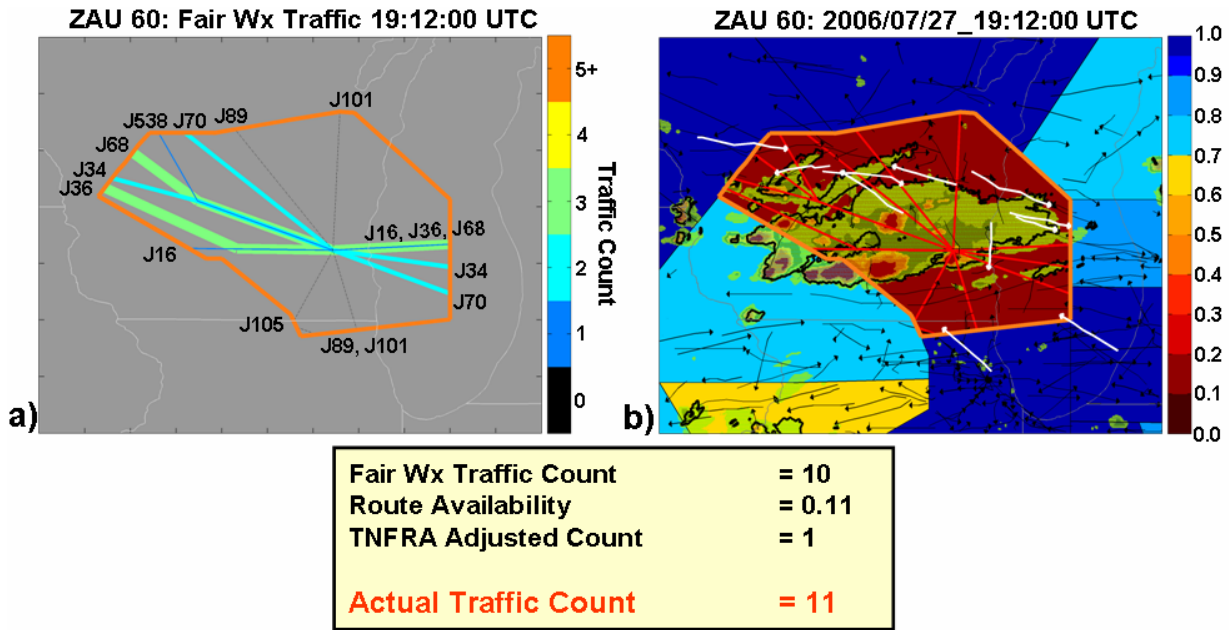


Figure 9. a) Fair weather estimates of traffic and shared traffic on routes in ZAU60 at 19:12 UTC. Routes are color coded by their traffic estimate as indicated by the colorbar to the right of the image. b) Convective weather impacts for ZAU60 on 27 July 2006 as indicated by the calculated TNFRA and colorbar to the right of the image. White trajectories indicate flights under the responsibility of ZAU60 controllers. Results for this instance show that actual traffic exceeds both the TNFRA and Fair weather estimates (box below a and b).

At 19:12 UTC, a broad cluster of intense convection lies along the southwestern facing boarder of ZAU60 (Fig. 9b). High Echo tops extend both horizontally and vertically into ZAU60 as indicated by the black 29 kft contour. WAF-pdps reached maxima of 90% for each of the level six convective cells seen impacting the sector. Given the intensity, vertical extent, and geographic location of convection with respect to heavily used routes in the sector, TNFRA is reduced to a value of 0.11, which translates to a traffic estimate of one aircraft. White trajectories in Fig.9b indicate an actual traffic count of 11. Clearly, in ZAU60, controllers have the option of vectoring traffic north outside of the usual operational bounds of the heavily impacted routes, without reducing capacity relative even to the sector's fair weather use.

Large differences between actual traffic and TNFRA estimates also occur when flows are redirected along unobstructed routes or into sectors typically in low demand. These instances make up a large portion of the positive outliers in the Δ distributions. Figure 10 provides an example of such an occurrence in ZMP02, a low altitude sector of the Minneapolis ARTCC. At 17:22 UTC, ZMP02 operates at a fair weather traffic volume of 5 aircraft. A small isolated convective cell impacts both the heavily used routes along the southern boarder of ZMP02 and the single north to south oriented route that runs down the center of the sector. The TNFRA estimate for ZMP02 at 17:22 UTC is 0.58, reducing the expected traffic count to 3 aircraft. The actual aircraft count exceeds the TNFRA estimate by 22 aircraft. The difference between actual traffic and estimated traffic persists for more than two hours. This is indicated by the 2 hour time series plot at the right of Fig. 10, showing the difference between the actual and TNFRA estimated traffic. The red line highlights the maximum difference, occurring at 17:22 UTC (+22 aircraft), and the time series indicates that differences greater than 5 aircraft between actual sector use and expected use as estimated by TNFRA occur throughout a full two hour period.

ZMP 02: 2006/07/27_17:22:00 UTC

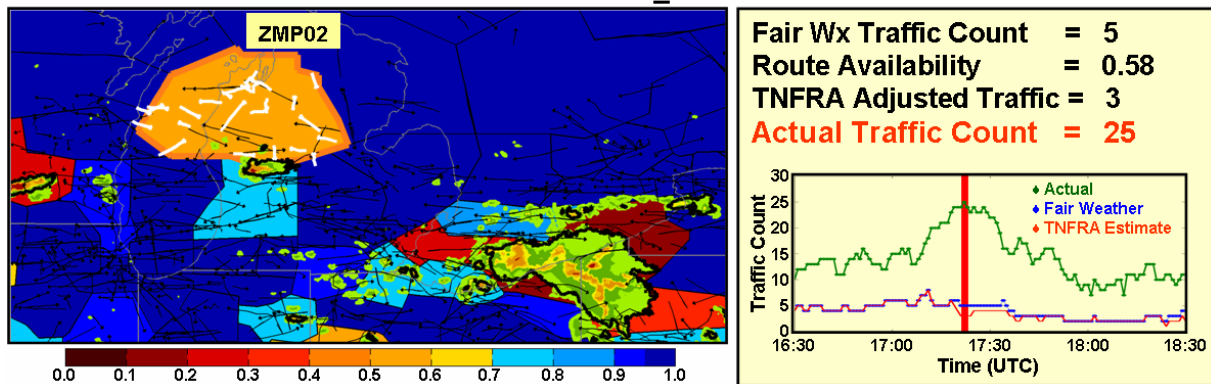


Figure 10. Differences in actual traffic and TNFRA estimated traffic that result from shifts in demand from highly impacted routes and sectors to routes and sectors typically in low demand. Left, ZMP02 at 17:22 UTC 27 July 2006 with a TNFRA estimate of 0.58. White trajectories indicate aircraft under responsibility of ZMP02 controllers. Right, comparison of actual traffic to fair weather estimates and TNFRA estimates. Red highlighted portion of the time series indicates the 17:22 UTC instance that corresponds to the maximum observed difference between actual traffic and estimated traffic.

The differences between actual traffic and the TNFRA estimates observed in ZMP02 are the result of weather-avoiding traffic reroutes that were in effect for much of the day. When convective weather impacts are significant in the Cleveland ARTCC, extensive reroutes to the north and south are put into place. Throughout much of the case day studied, east-west en route traffic that normally crosses the Cleveland ARTCC was rerouted through ZMP02, onto unobstructed routes, resulting in a vast increase in traffic relative to the average TNFRA demand. An examination of the tails of the Δ distributions in Fig. 7 reveals that differences between actual traffic and estimated traffic for ZMP02 make up 58% of the $+\Delta$'s that exceed 10 aircraft and 99.9% of the $+\Delta$'s of at least 15 aircraft.

Since TNFRA does not take into account distortions of the average clear weather demand due to weather-avoiding reroutes, this result is not surprising; TNFRA estimates sector capacities assuming regular ATC sector operations. TNFRA does not provide an estimate of achievable capacity where reroutes and other responses to convective weather result in a demand that is significantly different from the normal traffic weighting used in TNFRA, or where flights are allowed to deviate into airspace that is beyond the boundaries of the defined routes. TNFRA may be used as a metric to describe the severity of weather impact over a large region, or as a predictor of potential sector capacity overloads given an estimate of demand. ATC schedule optimization algorithms, such as those described in Bertsimas and Stock-Patterson⁸ and Weber et al⁹, may use the un-normalized route availability or TNFRA sector capacity estimates based on predicted demand to estimated airspace capacity in convective weather.

Local effects such as those shown in the three examples above contribute to the tails of the Δ distributions. However, TNFRA provides a good approximation of the wide-area impacts. Figure 11 is a time-series plot showing the instantaneous fair weather (blue), actual (green) and TNFRA-estimated (red) traffic counts, summed over the CIWS domain for 27 July 2006.

Fig. 11a shows that all three measures trend similarly from 01:00 UTC to the first local maximum in traffic count at 13:00 UTC. From 13:00 UTC to 17:00 UTC, actual CIWS wide demand exceeds both the fair weather and TNFRA estimates. Around 17:00 UTC, significant convective weather begins to appear in the CIWS domain (evidenced by the decrease in TNFRA traffic estimates), but impacts on actual traffic are not felt until about 19:00 UTC, when actual traffic counts begin to decline to levels well below the fair weather averages. From 21:00 UTC onward, TNFRA traffic estimates match actual traffic counts well.

Figure 11b shows a sub sample of the CIWS domain traffic comparing actual traffic counts with TNFRA estimates in ATC sectors experiencing no weather impact ($\overline{RA}=1$, TNFRA estimate = fair weather average). Throughout the event, the total traffic in all weather-free sectors was essentially the same as the clear weather average, suggesting that all of the capacity losses occurred in weather-impacted sectors and that little of that lost capacity (on average) was regained by increased throughput in weather-free sectors.

Figure 11c shows the traffic counts in sectors with any weather impacts ($\overline{RA}<1$), illustrating the good agreement between actual traffic and TNFRA estimates beyond 21:00 UTC.

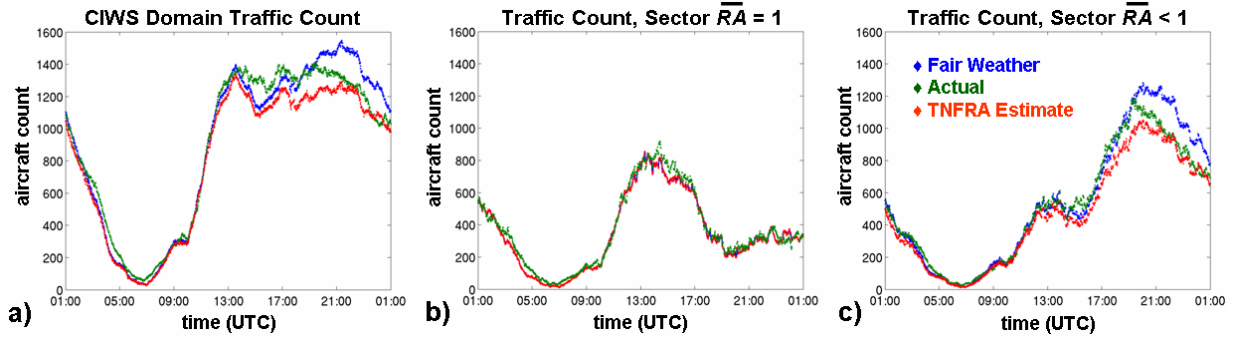


Figure 11. One minute counts of fair weather traffic (blue), actual traffic (green), and TNFRA estimated traffic (red) for the 27 July 2006 event. Counts are shown for a) all traffic in the CIWS domain, b) traffic in unobstructed sectors ($\overline{RA} = 1$), and c) traffic in weather impacted sectors ($\overline{RA} < 1$).

IV: Conclusions

The focus of this paper has been to present a novel approach to estimating convective weather impacts on ATC sector operations. The developed impact metric, Traffic Normalized Fractional Route Availability ties traffic reduction estimates to Weather Avoidance Fields which give the probability that a pilot will deviate around convective weather at each pixel in the field, to specific route structures, and to route usage in ATC sectors. TNFRA-based traffic reductions were calculated for the 406 low, high, and super-high ATC sectors in the CIWS domain for the duration of a high impact convective weather event that occurred 27 July 2006. One minute TNFRA estimates of ATC sector traffic were then compared to the actual traffic for the convective weather event. Results show that TNFRA slightly over-estimated weather impacts, but more than half of the TNFRA sector traffic estimates were within ± 1 aircraft of observed traffic counts and large differences were rare. The two principal types of observed differences between TNFRA estimated sector traffic and actual traffic were the distortion of fair weather demand due to weather mitigation strategies (weather avoiding reroutes, ground stops, etc.) and tolerance of weather-avoiding deviations beyond the model's operational route boundaries. While differences were seen when comparing the TNFRA estimates to actual traffic counts at the local ATC sector scale, TNFRA provided a good estimate of weather impacts on en route traffic over the full CIWS domain.

V: Future Work

- Improve route definitions to better model the operational flexibility, complexity, and constraints that determine the tolerance for weather-avoiding deviation in an ATC sector.
- Incorporate findings of the second version of Convective Weather Avoidance Modeling (CWAM2) into the TNFRA estimate.
- Develop algorithms that estimate reductions in ascending and descending route traffic that result from weather impacts.
- Couple TNFRA to a dynamic demand model that accounts for distortions of fair weather demand due to weather mitigation strategies.
- Expand the ATC sector fair weather demand database to cover the continental US.
- Validate TNFRA on additional cases.

References

- ¹DeLaura, R.A. and Evans, J.E., “An Exploratory Study of Modeling En Route Pilot Convective Storm Flight Deviation Behavior”, *American Meteorological Society, 12th Conference on Aviation, Range, and Aerospace Meteorology*, Atlanta, GA., 2006, Paper P12.6
- ²Evans, J. E., and Ducot E.R., “Corridor Integrated Weather System”, *Lincoln Laboratory Journal*, Vol. 16, No. 1, 2006 pp. 59-80.
- ³Welch, J.D., J. Andrews, B. Martin, B. Sridhar, 2007: “Macroscopic Workload Model for Estimating En Route Sector Capacity”, *7th Eurocontrol/FAA ATM R&D Seminar ATM-2007*, Barcelona, Spain, July 2007.
- ⁴Mitchell, J. S. B., Polishchuk V., Krozel J., “Airspace Throughput Analysis Considering Stochastic Weather”, *AIAA Guidance, Navigation, and Control Conference and Exhibit*, Keystone, 2006-6770, CO, Aug. 24-26, 2006.
- ⁵Song, L. Wanke, C., Greenbaum, D., “Predicting sector Capacity For TFM”, *7th Eurocontrol/FAA ATM R&D Seminar ATM-2007*, Barcelona, Spain, July 2007.
- ⁶Hunter, G., Raymamoorthy, K., Singnor, D. B., Post, J., “Evaluation of the Future National Airspace System in Inclement Weather”, *5th AIAA Aviation Technology, Integration and Operations Conference (ATIO)*, 2005-7449, Arlington, VA, Sep. 26-28, 2005.
- ⁷Federal Aviation Administration, “Aeronautical Information Manual: Official Guide to Basic Flight Information and ATC Procedures”, Department of Transportation: Federal Aviation Administration, Feb. 16, 2006.
- ⁸Bertsimas, D. and S. Stock-Patterson: “The Air Traffic Flow Management Problem with En Route Capacities, Operations Research”, 46, 406-422. , 1998
- ⁹Weber, M., J. Evans, M. Wolfson, R. DeLaura, W. Moser, B. Martin, D. Bertsimas, J. Welch and J. Andrews, “Improving Air Traffic Management during Thunderstorms”, *Digital Avionics System Conference (DASC)*, Washington, DC, 2005